

# COATINGS

UDC 621.793.6:678.026.34

## THE EFFECT OF DIAMOND BURNISHING ON STRUCTURE AND PROPERTIES OF DETONATION-GAS COATINGS ON GAS-TURBINE ENGINE PARTS

V. A. Boguslaev,<sup>1</sup> V. K. Yatsenko,<sup>2</sup> V. G. Yakovlev,<sup>3</sup> L. P. Stepanova,<sup>2</sup> and G. V. Pukhal'skaya<sup>2</sup>Translated from *Metallovedenie i Termicheskaya Obrabotka Metallov*, No. 1, pp. 47–51, January, 2008.

---

A diamond burnishing procedure for detonation coatings made from powder alloys PKKhN-15 and VKNA of parts made of steel Kh12NMBFSh is selected and substantiated, which ensures a favorable combination of the surface layer structure and properties.

---

### INTRODUCTION

The reliability and service life of gas-turbine engines (GTE) to a larger extent depend on the carrying capacity of their most loaded parts, such as blades, spindles, etc. A promising line in increasing the carrying capacity of GTE parts is detonation-gas spraying [1] and subsequent strain hardening. The possibility of strengthening parts by means of complex treatment makes detonation coatings especially topical.

The carrying capacity of a GTD spindle to a large extent is determined by the state of its surface layer, which is formed at the finish process stages. The quality of a detonation coating mainly depends on the properties and granulometric compositions of deposited powder materials: PKKhN-15 and VKNA.

The final treatment currently used for parts with detonation coatings is grinding. This technique ensures the required surface precision and roughness, but is accompanied by the formation of an unstable surface layer, frequently with tensile stresses or structural transformations impairing the carrying capacity of the material. Furthermore, grinding leaves deep traces acting as perceptible stress concentrators, which impairs the surface microrelief. A more effective method for finish treatment of parts (spindles) is diamond burnishing.

The purpose of the present paper is to investigate the effect of diamond burnishing on the structure, phase composition, roughness parameters, strain hardening, and residual stresses in detonation coatings on parts made of steel Kh12NMBF-Sh (ÉP-609).

### METHODS OF STUDY

In order to investigate diamond burnishing regimes for detonation coatings made from powders of alloys PKKhN-15 and VKNA (hereafter named simply coating PKKhN-15 and coating VKNA), sleeves were produced from steel Kh12NMBF-Sh (0.17–0.23% C, 10.5–12.5% Cr, 0.5–0.9% Ni, 0.5–0.7% Mo, 0.2–0.4% Mn, 0.15–0.30% V) with outer diameter of 104.75 mm and wall thickness of 3 mm. The external surfaces of the sleeves were finished by turning ( $R_a = 1.6$  mm). The chemical compositions of the powders for detonation spraying are listed in Table 1.

Before detonation spraying, the surfaces were treated by sand-blasting. The detonation coating thickness after its deposition and subsequent grinding on an abrasive wheel was 0.2 mm. The force  $P_y$  in burnishing varied from 100 to 400 N, and the feed varied from 0.04 to 0.12 mm/rev. The burnishing speed was 90 m/min. Hardening was performed in a single pass using I-20A oil.

The adhesion strength of the coating was determined using special blocks fastened in the gripping jaws of the R-0.5 breaking machine with the active grip migration velocity of 0.1 mm/min. Testing was performed on a set of at least four

---

<sup>1</sup> Motor Sich JSC, Zaporozhe, Ukraine.

<sup>2</sup> Zaporozhe National Technical University, Zaporozhe, Ukraine.

<sup>3</sup> Motor Sich JSC, Volochisk Machine-Building Works, Volochisk, Khmel'nitskii Oblast', Ukraine.



**Fig. 1.** A ring cut out from a sleeve and a sample for analysis cut across the ring generatrix.

samples after spray deposition, grinding, and diamond burnishing hardening. The tearing force  $Q$  and the adhesion strength  $\sigma_{ad}$  were determined based on the averaged values.

Residual stresses were determined on rings of width 10 mm cut out from the sleeves; the residual deformation of the ring was measured after cutting it across the generatrix (Fig. 1) using the following formula [3]:

$$\sigma_{cut} = \frac{2}{1-\mu} \frac{E \delta_{cut}}{D_{av}^2} \left( \frac{h}{2} - a \right),$$

where  $\mu = 0.3$  is the Poisson coefficient;  $E = 2.04 \times 10^5$  MPa is the elasticity modulus of steel Kh12NMBF-Sh;  $D_{av} = 101.75$  mm is the average diameter of the sleeve;  $\delta_{cut}$  is the change of the sample (ring) diameter after cutting;  $h = 3$  mm is the sample (ring) thickness;  $a$  is the current thickness of the surface layer.

To determine  $\delta_{cut}$  on the “Prismo” coordinate-measuring machine (Zeiss), the rings cut out from the sleeves and cut across the generatrix were subjected to spinning. Based on the spinning results we obtained the altered diameter value calculated using the rule of the minimum sum of the squares of the coordinate point deviation from the circumference. The residual stresses were calculated for  $a = 0$ , i.e., the stress level was determined at the sprayed layer surface.

To estimate the effect of the burnishing regimes on the level of microstresses, we determined the broadening  $\Delta\beta$  of nickel line (331) in coating PKKhN-15 on samples after diamond burnishing. The broadening  $\Delta\beta$  was determined with

**TABLE 2.** Adhesion Strength  $\sigma_{ad}$  and Tearing Force  $Q$  of Coating PKKhN-15 (Numerator) and Coating VKNA (Denominator) after Grinding (Initial) and after Diamond Burnishing

$P_y, N$	$S, mm/rev$	$Q, N$	$\sigma_{ad}, MPa$
Grinding	–	16.7; 16.7; 16.7; 22.7 (18.2)	$\frac{6}{6}$
		21; 17; 21; 19 (19.5)	$\frac{6}{6}$
200	0.08	26.7; 30; 24; 23.3 (26.0)	$\frac{8}{11}$
		31; 32; 34; 40 (34.25)	$\frac{10}{20}$
300	0.08	32; 40; 24.7; 30 (31.7)	$\frac{12}{25}$
		33; 60; 90; 70 (63.25)	$\frac{12}{25}$
400	0.08	33.3; 40.7; 36.7; 36.9 (36.9)	$\frac{12}{25}$
		70; 90; 83; 72 (78.75)	$\frac{12}{25}$

**Note.** Averages values of tearing force  $Q$  are indicated in brackets.

respect to the annealed state; for this purpose one of the samples was annealed for 1 h at 600°C to remove stresses. The line broadening was calculated according to the method described in [4].

The microstructure of the coatings was studied on the end sections of the sleeve samples.

The porosity of coatings PKKhN-15 and VKNA was determined by the linear method on microprofiles and estimated based on the porosity coefficient (index), i.e., the ratio of the total pore length to the calculation line length:

$$I_p = \frac{\sum l_p}{l}.$$

To reveal the structural specifics of detonation coatings, x-ray diffraction analysis was performed on a DRON-1 diffractometer in monochromatic copper radiation with data registration and processing on a computer linked to the diffractometer. The recording of the coating was performed from a plane parallel to the sample surface.

## RESULTS AND DISCUSSION

The most significant increase in the adhesion strength of coatings PKKhN-15 and VKNA was observed when the burnishing force  $P_y$  grew to 300 N with the feed  $S = 0.08$  mm/rev.

The results of adhesion strength tests (Table 2) indicated that the maximum increase in  $\sigma_{ad}$  is achieved within the interval  $P_y = 200 - 300$  N.

**TABLE 1.** Chemical Composition of Powders for Detonation Spraying

Powders	Content of elements, wt.%							
	Al	Ni	Cr	Ti	Co	Mo	W	Cr <sub>3</sub> C <sub>2</sub>
VKNA	26 – 28	Base	2.0 – 2.7	0.5	1.32	0.35	1.2	–
PKKhN-15	–	15	–	–	–	–	–	Base

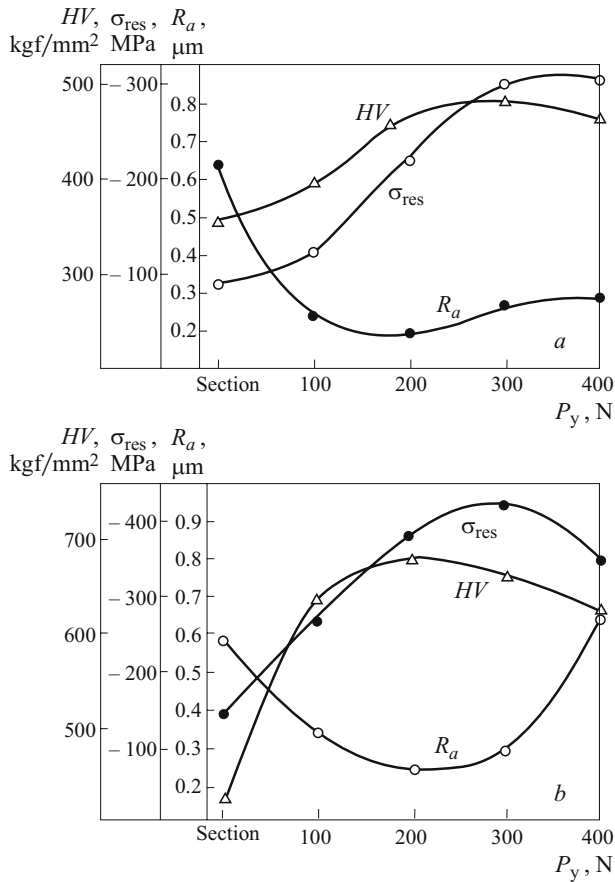


**Fig. 2.** Dependence of roughness  $R_a$ , microhardness  $HV$ , and residual stress  $\sigma_{res}$  on the force of diamond burnishing for coating VKNA (a) and coating PKKhN-15 (b).

The minimal roughness and the maximum microhardness and residual stress are observed in diamond burnishing with the force equal to 200 and 300 N (Fig. 2). Raising the burnishing force above 300 N is inadvisable. Thus, burnishing the coating VKNA with  $P = 400$  N resulted in exfoliation of the coating on certain sites of the sleeve due to excessive strain hardening.

It is known that among the surface layer properties (roughness, strain hardening, residual stress), residual compressive stress has the maximum impact on fatigue strength.

**TABLE 3.** Broadening ( $\Delta\beta$ ) of Nickel Line (331) (Coating PKKhN-15) and Iron Line (310) (the Sleeve) after Grinding (Initial) and after Diamond Burnishing

$P_y$ , N	$S$ , mm/rev	$\Delta\beta$ , rad	
		(331) Ni	(310) Fe
Grinding	—	$1.99 \times 10^{-2}$	$0.37 \times 10^{-2}$
100	0.08	$4.95 \times 10^{-2}$	$0.87 \times 10^{-2}$
200	0.08	$5.24 \times 10^{-2}$	$1.18 \times 10^{-2}$
300	0.08	$6.06 \times 10^{-2}$	$1.82 \times 10^{-2}$
400	0.08	$6.81 \times 10^{-2}$	$1.85 \times 10^{-2}$

It has been found that after diamond burnishing the highest residual compressive stress has been registered in coating PKKhN-15 (428 MPa), whereas the same stress in coating VKNA is equal to 296 MPa. At the same time, the microhardness of coating PKKhN-15 after burnishing (685  $HV$ ) is significantly higher than the microhardness of coating VKNA (495  $HV$ ).

Thus, the obtained results suggest that it is advisable to use a coating from powder PKKhN-15 for complex treatment of GTE spindles working under sign-variable loads.

The reason for the formation of microstresses in a coating is the plastic deformation of powder particles colliding with the base, as well as the effect of each subsequent coating layer on changes in the structure of the preceding layers [5].

It should be noted that the line broadening grows as the force  $P_y$  increases, which points to the growth of microstresses caused by the deformation processes in the coat layer under burnishing.

In the course of detonation spraying of coatings when particles collide with the base, the dislocation density in the surface layer can grow by three orders of magnitude and reach the value of  $4 \times 10^{11} \text{ cm}^{-2}$ , which causes the formation of stresses in the base.

The coating layers, which become cooled on the cold base, influence as well the microstress level. To reveal changes in the structure of the steel from which the sleeve is made and to estimate the effect of diamond burnishing on the sleeve surface layer, we obtained diffraction patterns of the end sections of the sample. The width of the slot restricting the x-ray section was 1 mm. In this recording scheme, the irradiated volume of the sample included both its coating around 200  $\mu\text{m}$  thick and the sleeve material.

It should be noted that in addition to the surface sites of the sleeve serving as the base for spray deposition of the coating, the diffraction patterns also encompasses other layers more remote from the surface; therefore, the surface area of the sleeve constitutes only a portion in the total irradiated surface.

Table 3 shows the broadening of ferrite line (310) obtained in recording diffraction patterns of the end surfaces of the samples. The ferrite line broadening is significantly smaller than the nickel line broadening in the coating. This is presumably due to the fact that the irradiated sample includes not only the surface zone but also the layers not reached by the deformation processes in burnishing.

Thus the burnishing process decreases roughness but increases microstresses both in the coating and in the surface layer of the sleeve, which indicates an increased dislocation density and a more complex dislocation structure.

The above conclusions are also corroborated by microhardness measurements data (Fig. 2). Thus, the microhardness of samples after diamond burnishing ( $P_y = 400$  N,  $S = 0.08$  mm/rev) grows nearly twice compared to its initial value.

Figures 3 and 4 show the microstructure of coatings after grinding and diamond burnishing on polished non-pickled

metallographic specimens and also on specimens after pickling in 4% solution of nitric acid in alcohol.

The contact zone of coating VKNA with the sleeve surface has an undular tortuous shape (for coating PKKhN-15 this is less so), which points to the deformation of the base after the deposition of this coating. Diamond burnishing levels the undulation of this boundary zone, which becomes more rectilinear. The structural components of coating VKNA are finely dispersed with weakly manifested boundaries between the layers, especially on the pickled specimens. Diamond burnishing decreases the roughness of the coating surface (Fig. 3).

Note that the existing single pores in the initial state have a round shape and after diamond burnishing they become more extended under the effect of the deformation force. The light-colored sites in coating PKKhN-15, which are presumably a nickel-based  $\alpha$ -solid solution, are small in the primarily layers of the coating and coarse only in the surface layer of the coating. As the force  $P_y$  in diamond burnishing grows, these sites become more extended, especially on the surface (Fig. 4). At a large magnification of the microstructure of coating PKKhN-15, in the darker-colored sites in all samples one can clearly identify fine rounded particles of a yellowish tint typical of chromium carbide particles. The  $\text{Cr}_2\text{C}_3$  phase has been identified in diffraction phase analysis.

Thus, the above structural specifics point to the deformation occurring in the material under burnishing.

It can be seen from Table 4 that the porosity of the coating after diamond burnishing under the optimum regime is actually half as much as after grinding and amounts to:  $I_p = 0.1175$  for coating PKKhN-15 and  $I_p = 0.1204$  for coating VKNA.

To reveal the structural specifics of the detonation coatings. X-ray diffraction analysis was carried out. The phase composition in the initial PKKhN-15 powder is represented by the lines of chromium carbide  $\text{Cr}_3\text{C}_2$  and nickel, which is used to clad the carbide particles. The phase composition of the coating PKKhN-15 changes little compared to the initial powder. It should be noted that the carbide  $\text{Cr}_3\text{C}_2$  lines are less intense than in the initial powder, which is due to the smaller irradiated volume of the coating and, possibly, a smaller number of carbide particles in the coating after detonation spraying. A small amount of carbide  $\text{Cr}_7\text{C}_3$  is possible as well, which can be formed under partial burn-out of carbon.

The main components in the initial powder VKNA are nickel and aluminum. The diffraction pattern of the initial

powder VKNA exhibits the phases Ni and NiAl. This agrees with the data in [6] demonstrating that precisely these phases

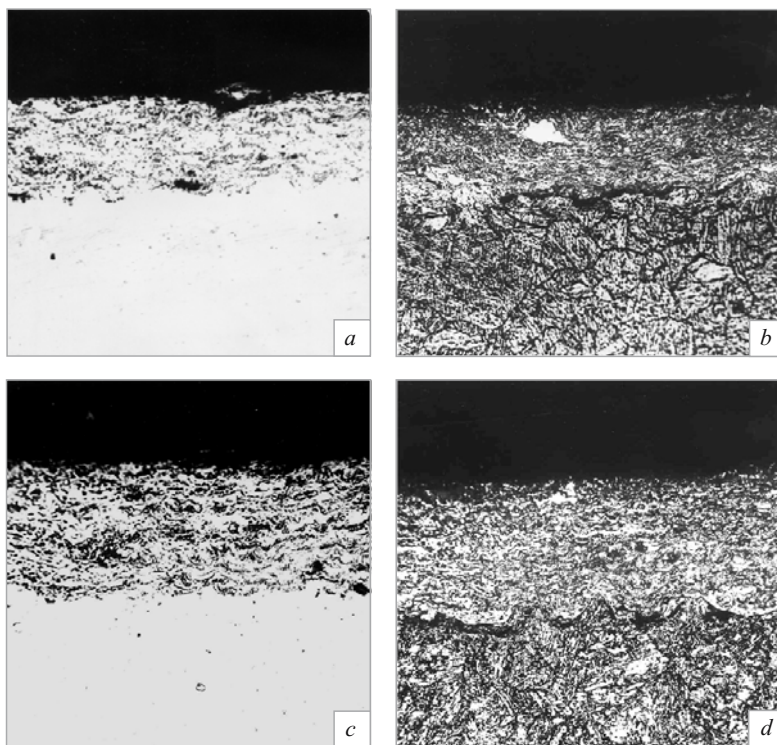


Fig. 3. Microstructure of coating VKNA after grinding on an elbow wheel (*a, b*) and after diamond burnishing with  $P_y = 300$  N (*c, d*),  $\times 200$ : *a, c*) polished sample; *b, d*) sample after pickling.

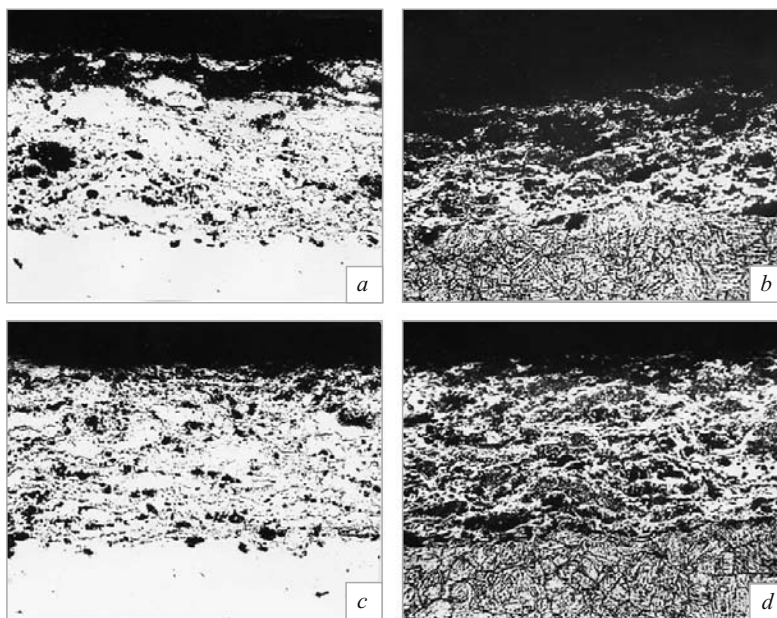


Fig. 4. Microstructure of coating PKKhN-15 after grinding on an elbow wheel (*a, b*) and after diamond burnishing with  $P_y = 300$  N (*c, d*),  $\times 200$ : *a, c*) polished sample; *b, d*) sample after pickling.

**TABLE 4.** Porosity  $I_p$  of Coatings on Steel Kh12NMBF-Sh

Coating	Fig. number	Treatment	$P_y$ , N	$S$ , mm/rev	$I_p$
VKNA	3a and b	Grinding	–	–	0.2105
	3c and d	Burnishing	300	0.08	0.1204
PKKhN-15	4a and b	Grinding	–	–	0.2309
	4c and d	Burnishing	300	0.08	0.1175

are observed in nickel-aluminum alloys containing over 17% Al.

In addition to the above phases, the coating sample VKNA also exhibits the lines of  $Ni_2Al$  and  $Ni_3Al$ . Analysis of the phase diagram of the Ni – Al system [7] shows that the phase  $Ni_3Al$  can exist in the form of single particles or within a eutectic consisting of the nickel-based  $\alpha$ -solid solution and the  $Ni_3Al$  phase formed from the liquid at 1385°C. The formation of these phases is possible in the course of the coating formation, when the detonation products temperature in the two-phase flow may reach several thousands degrees. The coating made from VKNA powder has a multiphase composition and includes the  $\alpha$ -solid Ni-based solution,  $NiAl$ ,  $Ni_3Al$ , and  $Ni_2Al_3$ .

Thus, the combined surface hardening of sleeves made of steel Kh12NMBF-Sh (detonation coating + diamond burnishing) decreases porosity, increases adhesion strength and microhardness, and raises the residual compressive stresses and microstresses, which leads to enhanced endurance parameters [8].

## CONCLUSIONS

1. Diamond burnishing of detonation coatings PKKhN-15 and VKNA performed with force  $P_y = 300$  N induces a more favorable combination of the surface layer

properties than grinding: adhesion strength grows 2 – 4 times, microhardness grows 2 times, surface roughness decreases 2 – 3 times, residual compressive stresses increase 2 – 3 times, which increases the carrying capacity of detonation-gas coatings.

2. The phase composition of coating PKKhN-15 is represented by chromium carbide  $Cr_3C_2$  and nickel which is used to clad the carbide particles. The coating made from powder VKNA has a multiphase composition including a nickel-based solid solution,  $NiAl$ ,  $Ni_3Al$ , and  $Ni_2Al_3$ .

## REFERENCES

1. A. I. Zverev, S. Yu. Sharivker, and E. L. Astakhov, *Detonation Spraying of Coatings* [in Russian], Sudostroenie, Leningrad (1979).
2. V. K. Yatsenko, G. Z. Zaitsev, and V. F. Pritchenko, et al., *Increasing the Carrying Capacity of Machine Parts by Diamond Burnishing* [in Russian], Mashinostroenie, Moscow (1985).
3. V. A. Boguslaev, V. G. Yakovlev, and V. P. Ben', "Technological specifics of complex hardening of GTE parts," *Vestn. Dvigatelistr.*, No. 1, 73 (2006).
4. S. S. Gorelik, L. N. Rastorguev, and Yu. A. Skakov, *X-ray Electron-Optical Analysis* [in Russian], Metallurgiya, Moscow (1970).
5. *Anticorrosion Coatings. Proc. All-Union Conf. on Heat-Resistant Coatings* [in Russian], Nauka, Leningrad (1983).
6. F. F. Khimushin, *Heat-Resistant Steels and Alloys* [in Russian], Metallurgiya, Moscow (1969).
7. N. P. Lyakishev (ed.), *Phase Diagrams of Binary Systems* [in Russian], Mashinostroenie, Moscow (1997 – 1998).
8. V. A. Boguslaev and V. G. Yakovlev, "Effect of combined treatment on fatigue resistance of GTE spindles," *Aviats.-Kosmich. Tekh. Tekhnol.*, No. 9(25), 68 – 72 (2005).